

Quantum back-action-evading gravitational wave detection in the negative mass reference frame

F.Ya.Khalili*

Faculty of Physics, M.V. Lomonosov Moscow State University, 119991 Moscow, Russia and

Russian Quantum Center, Skolkovo 143025, Russia

E.S.Polzik†

Niels Bohr Institute, University of Copenhagen, 2100, Denmark

Recent report on observation of gravitational waves [1, 2] has opened new horizons in cosmology and astrophysics. Gravitational wave detectors (GWD) such as LIGO and VIRGO are soon expected to be limited by the standard quantum limit (SQL) stemming from the balance between the measurement sensitivity and quantum back action. Recently a method to overcome the SQL for the measurement of motion by introducing a quantum reference frame in the form of an atomic spin oscillator has been demonstrated [3]. The method involves a joint measurement on the mechanical and spin systems, with the latter playing the role of a negative mass reference frame. Here we demonstrate how this novel approach can be used to overcome the SQL for the free mass, such as a mirror of a GWD. We present a general idea of the approach and provide the analysis of its experimental feasibility with realistic experimental parameters. We show that under realistic conditions the sensitivity of the GWD can be increased by 6 dB over the entire frequency band of interest. We also outline the ways to use the atomic system memory function for the benefit of GWD.

a. Introduction Sensitivity of state-of-the-art laser interferometric gravitational-wave detectors (GWD), such as Advanced LIGO [4], Advanced VIRGO [5], and GEO600 [6] is to a major extent limited by quantum fluctuations of the probing light. In the medium- and high-frequency range the sensitivity is dominated by the phase *shot noise* of light. In [7], Caves proposed to use a squeezed quantum state of light with reduced phase fluctuations to suppress the shot noise. Since 2011, this method is used in the GEO600 GW detector [8, 9]

According to the Heisenberg uncertainty relation, suppression of the phase fluctuations leads to proportional increase of the amplitude ones, which perturbs the interferometer mirrors motion. This perturbation is known as the *radiation pressure noise* or the *quantum back action* (QBA) noise. The point of balance of those two kinds of quantum noise is known as the Standard Quantum Limit (SQL) [10].

Intensity of the radiation pressure noise increases at low frequencies, as the mechanical susceptibility of suspended mirrors of GW detectors, $\chi = -1/\Omega^2$, which can be treated as free masses in the relevant detectors' sensitivity band. Currently, this low-frequency band is dominated by technical (non-quantum) noise sources. However, when the second generation detectors, such as Advanced LIGO, reach their design sensitivity, the radiation pressure (QBA) noise will be one of the major components of the total low-frequency noise [11].

Suppression of both the shot noise and the QBA, and thus overcoming the SQL, requires more advanced methods than simple frequency-independent squeezing. Several such methods were

* khalili@phys.msu.ru

† polzik@nbi.ku.dk

Notation	Quantity	Value, Adv.LIGO	Value, 10-m
r	Squeezing factor	$\frac{\log 15}{2} \leftrightarrow 15$ db	
L	Interferometer arms length	4000 m	10 m
m	Mirrors mass	40 kg	0.1 kg
κ_I	Interferometer half-bandwidth	$2\pi \times 500$ Hz	$2\pi \times 2000$ Hz
I_c	Optical power circulating in each of the arms	840 kW	1 kW
$\Theta = \frac{8\omega_o I_c}{mcL}$	normalized optical power	$(2\pi \times 100)^3 \text{ s}^{-3}$	$(2\pi \times 575)^3 \text{ s}^{-3}$
Ω_S	Atomic system eigen frequency	$2\pi \times 3$ Hz	$2\pi \times 30$ Hz
γ_S	Atomic system damping rate	$2\pi \times 3$ Hz	$2\pi \times 30$ Hz

TABLE I. The main notations used throughout this paper

proposed, see *e.g.* review paper [12]. In particular, in [13] it was proposed to use frequency-dependent squeezing with the amplitude noise suppressed at lower frequencies and the phase noise — at the higher ones. In order to create this frequency dependence, the authors proposed to reflect the “ordinary” squeezed light from an additional *filter cavity*. The main problem with this method is that this cavity has to be very narrow-band one (a few hundreds of Hertz). This translates into very long (hundred meters or even kilometers) and therefore expensive cavities. This complication is circumvented in a recent paper [14] where an auxiliary optical mode of the GWD interferometer itself is used as an effective filtering cavity. This scheme utilizes two entangled beams generated by non-degenerate parametric down-conversion process which are injected into the main and the auxiliary optical modes. However, it still requires significant modification of the GWD core optics, namely, two independent schemes for injection and extraction of the entangled beams.

A different approach to combat the QBA of measurement of motion where an atomic spin ensemble is used as an auxiliary system, has been proposed in [15]. The atomic ensemble was shown to perform a transformation of the probing light identical to the one of a mechanical harmonic oscillator with an effective negative mass (or a negative eigen frequency). In a recent work [3] the QBA evading idea using a high frequency nanomechanical oscillator and a spin oscillator was demonstrated experimentally.

Here we show that the negative frequency atomic spin ensemble provides broadband quantum noise reduction for motion of free masses, such as the GWD mirrors. In principle, it could be used in both sequential [13] and entangled [14] configurations. However, due to the specific requirement for the wavelength of light probing the atomic spin system, only the second configuration is feasible for the contemporary GWDs.

We show that the spin system allows for a broadband sensitivity beyond the SQL for interferometers of a very different scale: the Advanced LIGO and a much smaller 10-meter Hannover prototype interferometer which is currently under construction [16].

b. The scheme. Measurement of space distortions caused by gravitational waves (GW) is performed by an optical interferometer with suspended end mirrors (Figure 1). In the absence of optical losses, with the interferometer tuned on resonance, the phase quadrature of the light mode exiting the interferometer, \hat{b}_1^s , measured by a homodyne detector is [12, 17]:

$$\hat{b}_1^s = \hat{a}_1^s + \frac{2\kappa_I \Theta \chi}{(\kappa_I - i\Omega)^2} \hat{a}_I^c + \frac{\sqrt{2\kappa_I \Theta}}{\kappa_I - i\Omega} \chi \frac{F_s + F_T}{\sqrt{\hbar m}} \quad (1)$$

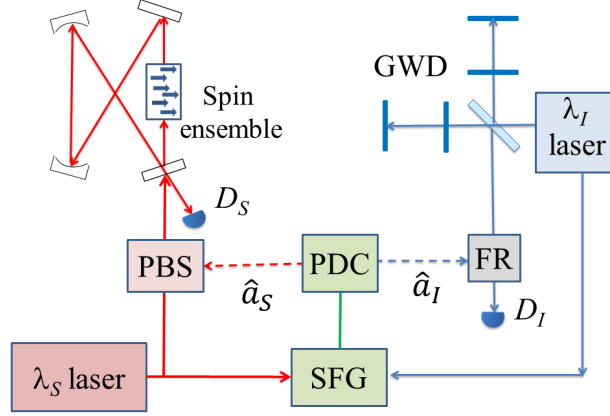


FIG. 1. **Setup for a GWD beyond the SQL with the negative mass spin system.** The GWD and the atomic system are probed with entangled light modes (dashed lines). Combined signals from detectors D1 and D2 allow for back action free measurement.

where \hat{a}_I^s, \hat{a}_I^c are the phase (sine) and amplitude (cosine) quadratures of the incident light, F_S is the signal force, for example from GW, and F_T is a sum of the thermal force, seismic noise and other technical noise sources (notations used throughout this paper are listed in the Table I). The first term describes the shot noise and the second one — the QBA noise.

If the incident light is in a coherent or in a squeezed state, then the quadratures \hat{a}_I^s, \hat{a}_I^c are uncorrelated and their spectral densities are equal to $e^{-2r}/2$ and $e^{2r}/2$. It is easy to show [7, 12] that in this case spectral density of the sum of the shot noise and QBA quantum noise (normalized to to signal force F_S) cannot be smaller than the force SQL $S_{\text{SQL}}^F = \hbar m \Omega^2$. Typically, it is recast as the equivalent position SQL:

$$S_{\text{SQL}}^x = \frac{S_{\text{SQL}}^F}{(m\Omega^2)^2} = \frac{\hbar}{m\Omega^2}. \quad (2)$$

Let us now introduce the second quantum system consisting of a multi-atom spin ensemble. If the spins are optically polarized along a certain direction x the collective spin has a large average projection $J_x = |\langle \hat{J}_x \rangle|/\hbar \gg 1$ [15, 18]. Its normalized y, z quantum components form canonical oscillator variables $\hat{X}_S = \hat{J}_z/\sqrt{\hbar J_x}, \hat{P}_S = -\hat{J}_y/\sqrt{\hbar J_x}$, satisfying the commutation relation $[\hat{X}_S, \hat{P}_S] = i$. In terms of those variables, the Hamiltonian for the ensemble placed in magnetic field oriented along x becomes

$$\hat{H}_S = \hbar\Omega_S J_x - \frac{\hbar\Omega_S}{2}(\hat{X}_S^2 + \hat{P}_S^2), \quad (3)$$

where Ω_S is the Larmor frequency. The first term is an irrelevant constant energy offset due to the mean spin polarization. The second term is equivalent to the Hamiltonian of a mechanical oscillator \hat{H}_M with a *negative* mass and spring constant. Each quantum of excitation in the negative mass spin oscillator physically corresponds to a deexcitation of the inverted spin population from its highest energy level by $\hbar\Omega_S$. Preparation of the collective spin in the energetically lowest Zeeman state realizes instead a *positive* mass and spring constant spin oscillator.

Interaction of light with a spin in magnetic field placed inside a resonator with the finesse \mathcal{F} can be cast in the form similar to that for the mechanical oscillator (see Supplementary Information):

$$\hat{b}_S^s = \hat{a}_S^s + 2\theta_S \chi_S \hat{a}_S^c + \sqrt{2\theta_S} \chi_S \hat{f}_S, \quad (4)$$

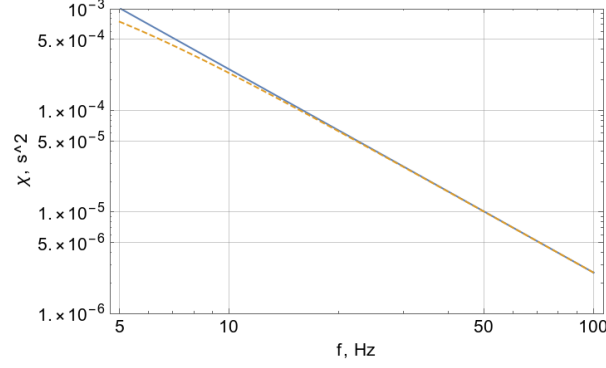


FIG. 2. Dashed line: susceptibility function χ for a free mass; solid line: absolute value of susceptibility of the spin system with $\Omega_S = \gamma_S = 2\pi \times 3$ Hz

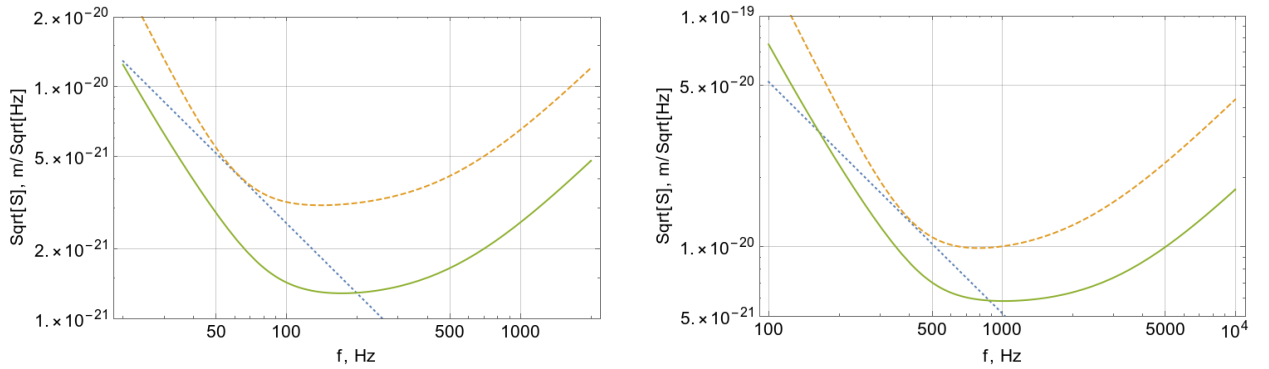


FIG. 3. **Spectral densities of quantum noise.** Dotted blue line - SQL; dashed orange curve - SQL-limited GWD noise; solid green curve - hybrid GWD/spin system. Left: Advanced LIGO, right: 10-m prototype (see Table I). In all cases, 2.5% of input losses and 2.5% of output losses are assumed for both GWD and atomic spin channels. In addition, 0.01% of intracavity roundtrip losses for the GWD are assumed.

where \hat{a}_S^s , \hat{a}_S^c are the phase (sine) and amplitude (cosine) quadratures of the input light mode in polarization orthogonal to the linearly polarized driving optical field, $\theta_S = \Omega_S \Gamma_S$, $\Gamma_S = \gamma_S d_0$ is the spin oscillator read out rate, $d_0 = \frac{\mathcal{F} \sigma N}{\pi A}$ is the cavity enhanced resonant optical depth of the spin ensemble, $\gamma_S = \frac{\sigma \gamma_{\text{opt}}^2 \Phi}{A \Delta_{\text{opt}}^2}$ is the spin bandwidth dominated by the optically induced decoherence, N is the atom number, σ - the atomic optical crosssection, A — the spin ensemble crosssection, γ_{opt} — optical transition bandwidth, Δ_{opt} - optical field detuning from atomic resonance, Φ — photon flux [3, 18],

$$\chi_S = (\Omega^2 - \Omega_S^2 + 2i\Omega\gamma_S)^{-1} \quad (5)$$

is the effective susceptibility of the spin oscillator, and \hat{f}_S is a normalized thermal force acting on the spin. An interesting and useful feature of a spin oscillator is that it is possible to provide the effective temperature of the noise \hat{f}_S close to zero even if the collective spin is formed by gas of atoms at room temperature [18]. Under such conditions the spectral density of this noise force corresponds to zero point fluctuations:

$$S_S = |\text{Im } \chi_S^{-1}| = 2|\Omega|\gamma_S. \quad (6)$$

The principle of the QBA evasion for measurement of motion using a spin as a negative mass reference frame has been demonstrated in [3]. There a light beam in a coherent state was used to sequentially probe the optomechanical system and the spin system, such that $\hat{a}_S^{c,s} = \hat{b}_I^{c,s}$ (note the similarity of this scheme with the one of [13], where light sequentially probes the test masses and the filter cavity). If the response of the spin system corresponds to the effective negative mass oscillator and matches the response of the interferometer, such that

$$\frac{\Theta\chi}{\kappa_I} = -\theta_S\chi_S, \quad (7)$$

then within the frequency band $\Omega < \kappa_I$ the QBA is cancelled in the output light mode:

$$\hat{b}_S^s = \hat{a}_I^s + \sqrt{\frac{2\Theta}{\kappa_I}} \chi \left(\frac{F_s + F_T}{\sqrt{\hbar m}} - \hat{f}_S \right), \quad (8)$$

resulting in the measurement sensitivity not limited by SQL.

For application of the negative spin mass idea to GW detectors the quantum light mode addressing the two systems cannot be the same because of the need to use very different wavelengths. The detectors are driven by $\lambda_I = 1064$ nm (and longer wavelengths are planned for the future), whereas the spin has to be driven by light nearly resonant to one of the strong atomic transitions, such as $\lambda_S = 852$ nm for Caesium [3].

A solution is to probe the GWD and the spin system with entangled light modes at $\hat{a}_I^{c,s}$ and $\hat{a}_S^{c,s}$ at wavelengths λ_I and λ_S , respectively. Such probe fields can be prepared by nonlinear optical transformations (sum frequency generation and parametric down conversion) as shown in Figure 1 [19]. A small fraction of the GW detector laser and a laser locked to the Caesium line generate a pump beam through the sum frequency generation in $\chi^{(2)}$ medium. This beam is then used to pump a parametric downconversion process (PDC) in which two-mode squeezed vacuum modes $\hat{a}_{I,S}$ at wavelengths λ_1 and λ_2 are generated [19, 20] satisfying

$$\hat{a}_{I,S}^c = \hat{z}_{I,S}^c \cosh r + \hat{z}_{S,I}^c \sinh r, \quad (9a)$$

$$\hat{a}_{I,S}^s = \hat{z}_{I,S}^s \cosh r - \hat{z}_{S,I}^s \sinh r. \quad (9b)$$

Here $\hat{z}_1^{c,s}$ and $\hat{z}_2^{c,s}$ correspond to two independent vacuum fields.

The sine quadratures $\hat{b}_{I,S}^s$ of the output beams are measured by the homodyne detectors $D_{I,S}$, respectively. Adding the output of the detector D_S , multiplied by the optimal weight function, to the output of D_I , we obtain the readout with the suppressed quantum noise. It is easy to show (SI) that in the ideal lossless case, the weight factor is equal to $\tanh 2r$, giving the noise suppression factor equal to $\cosh 2r$. Importantly, the lasers λ_I and λ_S do not have to be phase locked to each other. Rather only the phases between the local oscillators and the respective laser beams should be stabilized, so that the correct quadratures are detected.

c. Numerical estimates. The quantum noise spectral density of the considered scheme is calculated in the SI, taking into account the optical losses in the interferometer and the spin system for two sets of parameter, one of which approximately corresponds to the design goals of the Advanced LIGO [11] and the other one — to the Hannover 10-m prototype interferometer [16, 21], see Table I.

The critical parameters of the spin system are deduced from condition (7) using the parameters of the corresponding GWDs. Consider, for example, the Advanced LIGO interferometer. Its projected circulating power (Table I) corresponds to the normalized power $\Theta/(2\pi)^3 \approx (100 \text{ Hz})^3$

with the interferometer bandwidth $\kappa_I/2\pi \approx 500$ Hz [11]. Tuning the Larmor frequency of spins to $\Omega_S/2\pi = 3$ Hz, we arrive at the requirement for $\Gamma_S/2\pi \approx 600$ Hz. Note that from eq. (4) we can infer that on resonance the ratio of the ground state noise contribution (last term) to the shot noise is equal to half the ratio of the QBA (second term) to the ground state noise and is given by $\Gamma_S/\gamma_S = d_0$. In [22] we achieved this ratio and hence the $d_0 \approx 2$ for a single pass interaction in the atomic cells with the length of 4 cm. Increasing the length of the cell to 10 cm and placing the spin ensemble in an optical resonator with the finesse of $\mathcal{F} \approx 150$ will provide $d_0 \approx 200$. The 25 mm room temperature Caesium cells with advanced wall coating [18, 23] have the intrinsic linewidth < 1 Hz. With optical power broadening to $\gamma_S/2\pi = 3$ Hz we will be dominated by the meter readout and will achieve the required value of Γ_S/γ_S . In Figure 2, we plot the susceptibility functions for a free mass and for the spin system which are well matched to each other over the entire frequency band of interest.

In the 10-m prototype GWD case, the best sensitivity frequency band is shifted to upper frequencies by about one order of magnitude, which relaxes requirements for Ω_S , γ_S proportionally, see Table I. In this case, the required parameters are $\Gamma_S/2\pi \approx 3000$ Hz, $d_0 \approx 100$ and $\mathcal{F} \approx 75$.

In Figure 3, the resulting quantum noise spectral densities calculated in SI are shown for realistic optical losses listed in the figure caption. It follows from these results that the proposed scheme allows to implement the sensitivity gain about 6 db across the entire sensitivity band of interest.

d. Conclusion. We present a way to suppress quantum noise in gravitational wave interferometers by adding a spin oscillator into the detection path. The proposed method allows for broadband detection sensitivity beyond the Standard Quantum Limit across the entire frequency bandwidth relevant for gravitational wave observation. In comparison to the earlier proposals for beyond the SQL GWD which use either an external filtering cavity [13] or utilize the GW interferometer as an effective filtering cavity [14] our approach has an advantage of being completely compatible with existing GWDs and thus not requiring any complex and costly alterations in the GWD's core optics. It also paves the road towards generation of an entangled state of the multi-kilogram GWD mirrors and atomic spins which would be of fundamental interest due to the sheer size of the objects involved.

ACKNOWLEDGMENTS

We acknowledge motivating discussions with Nergis Mavalvala. E.S.P acknowledges funding by the ERC grant INTERFACE and by ARO grant W911NF. F.K. acknowledges funding by the RFBR grants 16-52-10069 and 16-52-12031.

-
- [1] B. Abbott *et al*, Phys. Rev. Lett. **116**, 061102 (2016).
 - [2] B. Abbott *et al*, Phys. Rev. Lett. **116**, 241103 (2016).
 - [3] C. B. Møller *et al.*, Nature **547**, 191 (2017).
 - [4] <http://www.ligo.caltech.edu>.
 - [5] <http://www.virgo-gw.eu>.
 - [6] <http://www.geo600.org>.
 - [7] C. M. Caves, Phys. Rev. D **23**, 1693 (1981).
 - [8] J. Abadie *et al*, Nature Physics **7**, 962 (2011).
 - [9] H. Grote *et al.*, Phys. Rev. Lett. **110**, 181101 (2013).

- [10] V.B.Braginsky, F.Ya.Khalili, *Quantum Measurement*, Cambridge University Press, 1992.
- [11] J.Aasi *et al*, *Classical and Quantum Gravity* **32**, 074001 (2015).
- [12] S.L.Danilishin, F.Ya.Khalili, *Living Reviews in Relativity* **15** (2012).
- [13] H.J.Kimble, Yu.Levin, A.B.Matsko, K.S.Thorne and S.P.Vyatchanin, *Physical Review D* **65**, 022002 (2001).
- [14] Y. Ma *et al.*, *Nature Physics* **13**, 776 (2017).
- [15] K. Hammerer, M. Aspelmeyer, E. S. Polzik, and P. Zoller, *Phys. Rev. Lett.* **102**, 020501 (2009).
- [16] http://www.aei.mpg.de/18478/04_10m_Prototype.
- [17] A.Buonanno, Y.Chen, *Physical Review D* **67**, 062002 (2003).
- [18] K. Hammerer, A. S. Sørensen, and E. S. Polzik, *Rev. Mod. Phys.* **82**, 1041 (2010).
- [19] C. Schori, J. L. Sørensen, and E. S. Polzik, *Phys. Rev. A* **66**, 033802 (2002).
- [20] N. P. Georgiades, E. S. Polzik, K. Edamatsu, H. J. Kimble, and A. S. Parkins, *Phys. Rev. Lett.* **75**, 3426 (1995).
- [21] Tobias Westphal *et al*, arXiv:1111.7252 (2011).
- [22] W. Wasilewski *et al.*, *Phys. Rev. Lett.* **104**, 133601 (2010).
- [23] M. V. Balabas *et al.*, *Opt. Express* **18**, 5825 (2010).

Notation	Quantity	Value
η_{I1}	quantum efficiency of the input path of the interferometer	97.5%
η_{I3}	quantum efficiency of the output path of the interferometer	97.5%
A_I	Light absorption per bounce in the interferometer	0.01%
$\kappa_{I1} = \eta_{I2}\kappa_I = \frac{cA_I}{4L}$	part of the interferometer half-bandwidth due to the optical losses	
$\kappa_{Ic} = (1 - \eta_{I2})\kappa_I$	part of the interferometer half-bandwidth due to the coupling	
η_{S1}	quantum efficiency of the input path of the spin system system	97.5%
η_{S3}	quantum efficiency of the output path of the atomic system	97.5%
A_S	Light absorption per bounce in the spin system	
L_S	Length of the spin system cavity	
$\kappa_{S1} = (1 - \eta_{S2})\kappa_S = \frac{cA_S}{4L_S}$	part of the spin system cavity half-bandwidth due to the optical losses	
$\kappa_{Sc} = \eta_{S2}\kappa_S$	part of the atomic system cavity half-bandwidth due to the coupling	

TABLE II. Notation related to the optical losses

SUPPLEMENTARY INFORMATION

1. Input/output relation

With optical losses taken into account, Eqs. (1, 4) of the main text can be shown [s1, s2] to take the following form:

$$\hat{b}_I^s = \sqrt{\eta_{I3}} \left[\mathcal{R}_I \hat{c}_I^s + \frac{2\kappa_{Ic}\Theta\chi}{\ell^2} \hat{c}_I^c + \mathcal{T}_I \left(\hat{n}_{I2}^s + \frac{\Theta\chi}{\ell} \hat{n}_{I2}^s \right) + \sqrt{\frac{2\kappa_{Ic}\Theta}{\hbar m}} \frac{\chi F_s}{\ell} \right] + \sqrt{1 - \eta_{I3}} \hat{n}_{I3}, \quad (10a)$$

$$\hat{b}_S^s = \sqrt{\eta_{S3}} \left[\mathcal{R}_S \hat{c}_S^s + 2\eta_{S2}\theta_S\chi_S \hat{c}_S^c + \mathcal{T}_S (\hat{n}_{S2}^s + \theta_S\chi_S \hat{n}_{S2}^c) + \sqrt{2\eta_{S2}\theta_S} \chi_S f_S \right] + \sqrt{1 - \eta_{S3}} \hat{n}_{S3}, \quad (10b)$$

Here

$$\hat{c}_I^{c,s} = \sqrt{\eta_{I1}} \hat{a}_I^{c,s} + \sqrt{1 - \eta_{I1}} \hat{n}_{I1}^{c,s}, \quad (11a)$$

$$\hat{c}_S^{c,s} = \sqrt{\eta_{S1}} \hat{a}_S^{c,s} + \sqrt{1 - \eta_{S1}} \hat{n}_{S1}^{c,s} \quad (11b)$$

are the effective incident light quadratures for the interferometer and the spin system cavity, $\hat{n}_{I1}^{c,s}$ and $\hat{n}_{I3}^{c,s}$, $\hat{n}_{S1}^{c,s}$ and $\hat{n}_{S3}^{c,s}$ are the vacuum noise operators associated with the input and the output losses, $\hat{n}_{S2}^{c,s}$, $\hat{n}_{I2}^{c,s}$ are the vacuum noise operators due to the internal optical losses in the interferometer/spin system cavity,

$$\ell = \kappa_I - i\Omega, \quad (12a)$$

$$\mathcal{R}_I = \frac{2\kappa_{Ic}}{\ell} - 1, \quad \mathcal{T}_I = \frac{2\sqrt{\kappa_{Ic}\kappa_{I1}}}{\ell}, \quad (12b)$$

$$\mathcal{R}_S = \frac{\kappa_{Sc} - \kappa_{S1}}{\kappa_S}, \quad \mathcal{T}_S = \frac{2\sqrt{\kappa_{Sc}\kappa_{S1}}}{\kappa_S}. \quad (12c)$$

Other notations are listed in Table II.

It follows from (10a) that the signal force estimate without detection on the spin system is given by

$$\tilde{F}_{sI} = \sqrt{\frac{\hbar m}{2\kappa_{Ic}\Theta}} \frac{\kappa_I - i\Omega}{\chi} \hat{b}_I^s = F_s + \hat{F}_I, \quad (13)$$

where

$$\hat{F}_I = \sqrt{\frac{\hbar m}{2\kappa_{Ic}\Theta}} \frac{\ell}{\chi} \left[\mathcal{R}_I \hat{c}_I^s + \frac{2\kappa_{Ic}\Theta\chi}{\ell^2} \hat{c}_I^c + \mathcal{T}_I \left(\hat{n}_{I2}^s + \frac{\Theta\chi}{\ell} \hat{n}_{I2}^c \right) + \sqrt{\frac{1-\eta_{I3}}{\eta_{I3}}} \hat{n}_{I3} \right] \quad (14)$$

is the quantum noise in the interferometer channel alone.

2. Spectral densities

Spectral densities of the input noise components [see Eq. (9) of the main text] are defined by the degree of two-mode squeezing

$$S[\hat{a}_I^c] = S[\hat{a}_I^s] = S[\hat{a}_S^c] = S[\hat{a}_S^s] = \frac{\cosh 2r}{2}. \quad (15a)$$

The only non-zero cross-correlation spectral densities are

$$S[\hat{a}_I^c \hat{a}_S^c] = \frac{\sinh 2r}{2}, \quad S[\hat{a}_I^s \hat{a}_S^s] = -\frac{\sinh 2r}{2}. \quad (15b)$$

Therefore, spectral densities of $\hat{c}_{I,S}^{c,s}$ and their (non-zero) cross-correlation spectral densities are equal to, respectively

$$S[\hat{c}_I^c] = S[\hat{c}_I^s] = \frac{\rho_I + 1}{2}, \quad (16a)$$

$$S[\hat{c}_S^c] = S[\hat{c}_S^s] = \frac{\rho_S + 1}{2}, \quad (16b)$$

$$S[\hat{c}_I^c \hat{c}_S^c] = \frac{\rho_{IS}}{2}, \quad S[\hat{c}_I^s \hat{c}_S^s] = -\frac{\rho_{IS}}{2}, \quad (16c)$$

where

$$\rho_I = 2\eta_{I1} \sinh^2 r, \quad (17a)$$

$$\rho_S = 2\eta_{S1} \sinh^2 r, \quad (17b)$$

$$\rho_{IS} = \sqrt{\eta_{I1}\eta_{S1}} \sinh 2r. \quad (17c)$$

The force spectral densities for the interferometer and the spin system (14, 10b) and their cross-correlation spectral density are:

$$S_I = \frac{\hbar m |\ell|^2}{4\kappa_{Ic}\Theta |\chi|^2} \sigma_I, \quad (18a)$$

$$S_{\text{Spin}} = \frac{\eta_{S3}}{2} \sigma_{\text{Spin}}, \quad (18b)$$

$$S_{I\text{Spin}} = \frac{1}{2} \sqrt{\frac{\hbar m \eta_{S3}}{2\kappa_{Ic}\Theta}} \frac{\ell}{\chi} \sigma_{I\text{Spin}}. \quad (18c)$$

Here

$$\sigma_I = |\mathcal{R}_I|^2 \rho_I + \frac{1}{\eta_{I3}} + \frac{4\eta_{I2}\kappa_I^2\Theta^2|\chi|^2}{|\ell|^4}(\eta_{I2}\rho_I + 1), \quad (19a)$$

$$\sigma_{\text{Spin}} = \mathcal{R}_S^2 \rho_S + \frac{1}{\eta_{S3}} + 4\eta_{S2}\theta_S^2|\chi_S|^2(\eta_{S2}\rho_S + 1) + 4\eta_{S2}\theta_S|\text{Im } \chi_S|, \quad (19b)$$

$$\sigma_{\text{ISpin}} = \left(-\mathcal{R}_I\mathcal{R}_S + \frac{4\kappa_{Ic}\eta_{S2}\Theta\theta_S\chi\chi_S^*}{\ell^2} \right) \rho_{IS}. \quad (19c)$$

The force estimate for the hybrid interferometer-spin system is equal to

$$\tilde{F}_s = \tilde{F}_{sI} + \alpha \hat{b}_s^s, \quad (20)$$

where

$$\alpha = -\frac{S_{\text{ISpin}}}{S_{\text{Spin}}}. \quad (21)$$

The resulting effective position noise spectral density is equal to

$$S = |\chi|^2 \left(S_I - \frac{|S_{\text{ISpin}}|^2}{S_{\text{Spin}}} \right) = \frac{\hbar m |\ell|^2}{4\kappa_{Ic}\Theta} \left(\sigma_I - \frac{|\sigma_{\text{ISpin}}|^2}{\sigma_{\text{Spin}}} \right). \quad (22)$$

3. Asymptotic cases

a. Strong squeezing. Consider the leading in e^r terms in Eqs. (19). In this approximation,

$$\rho_I \approx \frac{\eta_{I1}e^{2r}}{2}, \quad (23a)$$

$$\rho_S \approx \frac{\eta_{S1}e^{2r}}{2}, \quad (23b)$$

$$\rho_{IS} \approx \frac{\sqrt{\eta_{I1}\eta_{S1}}e^{2r}}{2}, \quad (23c)$$

$$\sigma_I \approx \frac{\eta_{I1}e^{2r}}{2} \left(|\mathcal{R}_I|^2 + \frac{4\eta_{I2}^2\kappa_I^2\Theta^2|\chi|^2}{|\ell|^4} \right), \quad (24a)$$

$$\sigma_{\text{Spin}} \approx \frac{\eta_{S1}e^{2r}}{2} \left(\mathcal{R}_S^2 + 4\eta_{S2}^2\theta_S^2|\chi_S|^2 \right), \quad (24b)$$

$$\sigma_{\text{ISpin}} \approx \frac{\sqrt{\eta_{I1}\eta_{S1}}e^{2r}}{2} \left(-\mathcal{R}_I\mathcal{R}_S + \frac{4\eta_{I2}\eta_{S2}\kappa_I\Theta\theta_S\chi\chi_S^*}{\ell^2} \right). \quad (24c)$$

and

$$\sigma_I - \frac{|\sigma_{\text{ISpin}}|^2}{\sigma_{\text{Spin}}} \approx \frac{\eta_{I1}e^{2r}}{2} \frac{\left| \frac{\mathcal{R}_S\eta_{I2}\kappa_I\Theta\chi}{\ell^2} + \mathcal{R}_I\eta_{S2}\theta_S\chi_S \right|^2}{\mathcal{R}_S^2 + 4\eta_{S2}^2\theta_S^2|\chi_S|^2}. \quad (25)$$

In order to compensate the noise, the numerator of this equation has to be equal to zero. The simplified frequency-independent form of this condition is the following:

$$\frac{\eta_{S2}}{1 - 2\eta_{S2}} \theta_S = \frac{\eta_{I2}}{1 - 2\eta_{I2}} \frac{\Theta}{\kappa_I}. \quad (26)$$

b. Shot noise. Suppose that the shot noise dominates in Eqs. (19):

$$\sigma_I \approx |\mathcal{R}_I|^2 \rho_I + \frac{1}{\eta_{I3}}, \quad (27a)$$

$$\sigma_{\text{Spin}} \approx \mathcal{R}_S^2 \rho_S + \frac{1}{\eta_{S3}}, \quad (27b)$$

$$\sigma_{I\text{Spin}} \approx -\mathcal{R}_I \mathcal{R}_S \rho_{IS}. \quad (27c)$$

In this case,

$$\sigma_I - \frac{|\sigma_{I\text{Spin}}|^2}{\sigma_{\text{Spin}}} \approx \frac{2 \left(\frac{\mathcal{R}_S^2 \eta_{S1}}{\eta_{I3}} + \frac{|\mathcal{R}_I|^2 \eta_{I1}}{\eta_{S3}} - 2|\mathcal{R}_I|^2 \mathcal{R}_S^2 \eta_{S1} \eta_{I1} \right) \sinh^2 r + \frac{1}{\eta_{I3} \eta_{S3}}}{2\mathcal{R}_S^2 \eta_{S1} \sinh^2 r + \frac{1}{\eta_{S3}}}. \quad (28)$$

Then suppose that

$$\epsilon_{\alpha\beta} = 1 - \eta_{\alpha\beta} \ll 1, \quad \kappa_{II} \ll \kappa_I \Rightarrow |\mathcal{T}_I|^2 \ll 1 \quad \kappa_{SI} \ll \kappa_S \Rightarrow \mathcal{T}_S^2 \approx 4(1 - \eta_{S2}) = 4\epsilon_{S2} \ll 1, \quad (29)$$

and the squeezing is strong, $e^r \gg 1$. In this case, keeping only the first order non-vanishing loss terms amplified by squeezing, and neglecting those terms if they not enhanced by $\sinh^2 r$, we obtain:

$$\sigma_I - \frac{|\sigma_{I\text{Spin}}|^2}{\sigma_{\text{Spin}}} \approx \frac{2(\epsilon_{I1} + |\mathcal{T}_I|^2 + \epsilon_{I3} + \epsilon_{S1} + 4\epsilon_{S2} + \epsilon_{S3}) \sinh^2 r + 1}{\cosh 2r}. \quad (30)$$

c. Radiation pressure noise. Under condition of the radiation-pressure noise dominating other noise sources:

$$\sigma_I \approx \frac{4\eta_{I2} \kappa_I^2 \Theta^2 |\chi|^2}{|\ell|^4} (\eta_{I2} \rho_I + 1), \quad (31a)$$

$$\sigma_{\text{Spin}} \approx 4\eta_{S2} \theta_S^2 |\chi_S|^2 (\eta_{S2} \rho_S + 1), \quad (31b)$$

$$\sigma_{I\text{Spin}} \approx \frac{4\kappa_I \eta_{I2} \eta_{S2} \Theta \theta_S \chi \chi_S^*}{\ell^2} \rho_{IS}. \quad (31c)$$

In this case,

$$\sigma_I - \frac{|\sigma_{I\text{Spin}}|^2}{\sigma_{\text{Spin}}} \approx \frac{4\eta_{I2} \kappa_I^2 \Theta^2 |\chi|^2}{|\ell|^4} \times \frac{2(\eta_{I1} \eta_{I2} + \kappa_I \eta_{S1} \eta_{S2} - 2\eta_{I1} \eta_{I2} \eta_{S1} \eta_{S2}) \sinh^2 r + 1}{2\eta_{S2} \sinh^2 r + 1}. \quad (32)$$

Combining this result with assumptions (29), we obtain

$$\sigma_I - \frac{|\sigma_{I\text{Spin}}|^2}{\sigma_{\text{Spin}}} \approx \frac{4\kappa^2 \Theta^2 |\chi|^2}{|\ell|^4} \times \frac{2(\epsilon_{I1} + \epsilon_{I2} + \epsilon_{S1} + \epsilon_{S2}) \sinh^2 r + 1}{\cosh 2r}. \quad (33)$$

[s1] S.L.Danilishin, F.Ya.Khalili, Living Reviews in Relativity **15** (2012).

[s2] K. Hammerer, A. S. Sørensen, and E. S. Polzik, Rev. Mod. Phys. **82**, 1041 (2010).